

Organic & Biomolecular Chemistry

Accepted Manuscript



This is an *Accepted Manuscript*, which has been through the Royal Society of Chemistry peer review process and has been accepted for publication.

Accepted Manuscripts are published online shortly after acceptance, before technical editing, formatting and proof reading. Using this free service, authors can make their results available to the community, in citable form, before we publish the edited article. We will replace this *Accepted Manuscript* with the edited and formatted *Advance Article* as soon as it is available.

You can find more information about *Accepted Manuscripts* in the [Information for Authors](#).

Please note that technical editing may introduce minor changes to the text and/or graphics, which may alter content. The journal's standard [Terms & Conditions](#) and the [Ethical guidelines](#) still apply. In no event shall the Royal Society of Chemistry be held responsible for any errors or omissions in this *Accepted Manuscript* or any consequences arising from the use of any information it contains.

Marine Natural Products-Inspired Phenylmethylene Hydantoins with Potent *in Vitro* and *in Vivo* Antitumor Activities via Suppression of Brk and FAK Signaling

Asmaa A. Sallam^a, Mohamed M. Mohyeldin^a,
 Ahmed I. Foudah^a, Mohamed R. Akl^a, Sami Nazzal^a,
 Sharon A. Meyer^b, Yong-Yu Liu^a, Khalid A. El
 Sayed^{a*}

Received (in XXX, XXX) Xth XXXXXXXXX 20XX, Accepted
 Xth XXXXXXXXX 20XX

DOI: 10.1039/b000000x

Breast and prostate cancers are among the most common cancers worldwide with devastating statistics for the metastatic, chemotherapy- and radiotherapy-resistant phenotypes. Novel therapies interfering with new and/or multiple pathways involved in the pathology of cancer are urgently needed. Preliminary results found that the marine natural product Z-4-hydroxyphenylmethylene hydantoin (PMH, **1**) and its 4-ethylthio-analog (SEth, **2**) promoted tight junctions formation and showed anti-invasive and anti-migratory activities *in vitro* against metastatic prostate cancer cells and inhibited tumor growth and micrometastases in distant organs in orthotopic and transgenic mice models. This study focuses on the design and synthesis of second-generation PMHs with enhanced antitumor activities. A series of substituted benzaldehydes selected based on earlier SAR studies and reacted with hydantoin to yield 11 new compounds **3-13**. Compounds were evaluated for their antiproliferative, antimigratory and anti-invasive properties *in vitro* against the human mammary and prostate cancer cell lines MDA-MB-231 and PC-3, respectively. Western blot analysis of the most active analog **7** showed its ability to suppress the expression of the total levels of c-Met and FAK, with subsequent reduction in their phosphorylated (activated) levels in MDA-MB-231 cells. In addition, **7** also inhibited Brk, paxillin and Rac1 phosphorylation. **7** was formulated using hydroxypropyl β -cyclodextrin (HPCD) to improve its solubility and further evaluated in a nude mice xenograft model using MDA-MB-231/GFP cells. PMH **7** reduced breast tumor growth and suppressed Ki-67, CD31, p-Brk and p-FAK expression in tumor samples. Thus, **7** is a potential lead for the control of invasive breast malignancies.

Introduction

Breast cancer is the second most common cancer among American women after skin cancers.¹ About 1 in 8 (12%) women in the US will develop invasive breast cancer during their lifetime.¹ Similarly, prostate cancer is the most frequently diagnosed malignancy in adult men from western countries.² About 1 in 6 men will be diagnosed with prostate cancer during their lifetime.¹ Although the precise molecular mechanisms underlying the transformation of these cancers from the primary, treatment-responsive to the resistant and highly metastatic status remain largely unknown, lines of evidence have shown that aberrant receptor tyrosine kinase (RTK) signaling play a crucial

role.³ Understanding the signaling pathways involved in establishing a metastatic phenotype in cancer is fundamental for understanding the pathology and treatment of the disease.⁴ Aberrant tyrosine kinase signaling, whether by stimulation of growth factor receptors or intracellular tyrosine kinases expression, has been shown to contribute to various steps of tumor development and progression, including metastasis.⁴

c-Met is a receptor tyrosine kinase (RTK) that acts as the receptor for its only known ligand, hepatocyte growth factor (HGF) or scatter factor (SF).^{3,5} c-Met is expressed mainly in cells of mesenchymal origin, although some epithelial cancer cells appear to express both HGF and c-MET.³ The HGF/c-MET axis contributes a critical physiologic function in embryogenesis, angiogenesis, and wound healing.⁵ However, improper HGF/c-MET interaction may confer proliferative, survival, and invasive/metastatic abilities of cancer cells.^{3,5} The HGF/c-MET signaling cascade has been repeatedly shown to be dysregulated in a variety of tumors such as lung, kidney, head & neck, breast, prostate and colorectal cancers.⁵⁻⁷ Increased HGF/c-MET signaling in these tumors correlates with poor patient outcomes.^{5,7} In addition, phosphorylated c-MET has also been shown to be an important predictor of tumor aggressiveness, metastatic potential, and poor survival.⁵

Breast tumor kinase (Brk), also known as PTK6, is an intracellular tyrosine kinase related to Src family kinases that is typically expressed in differentiated epithelial cells of the skin and gastrointestinal tract.^{4,8-10} In normal breast epithelium, Brk is low or undetectable, but the protein is overexpressed in up to 86% of breast tumors, with the highest levels in advanced tumors, suggesting that Brk expression is related to carcinogenesis.^{9,10} Its expression levels increase in association with the carcinoma content of breast tumors, tumor grade, and invasiveness.⁸⁻¹⁰ Melanoma, lymphoma, ovarian, prostate, and colon cancers can also exhibit overexpressed and/or mis-localized Brk.¹⁰ Although the expression is not significantly altered in prostate cancer, Brk translocates from the nucleus to the cytoplasm during tumor progression.^{4,11}

Focal adhesion kinase (FAK), a non-receptor tyrosine kinase, is an important intermediary of growth factor signaling, cell survival, proliferation, adhesion, migration, and invasion.^{12,13} FAK has been shown to regulate cell migration and invasion through distinct pathways by promoting the dynamic regulation of focal adhesion and peripheral actin polymerization, as well as the matrix metalloproteinases (MMPs)-mediated extracellular matrix (ECM) degradation.¹⁴ Tyrosine phosphorylation of FAK also triggers downstream signaling events, including phosphorylation of paxillin, which is required for the cytoskeleton reorganization to facilitate cell metastasis.¹⁴ Elevated FAK expression has been observed in a number of human cancer cell lines and is well correlated with tumor development and/or the maintenance of tumor phenotype.^{12,15}

Paxillin is a multidomain adaptor protein primarily functioning as a molecular scaffold that provides multiple docking sites at the plasma membrane for an array of signaling, adaptor, and structural proteins.⁴ Through these interactions, paxillin is involved in a variety of physiological functions, including matrix organization, cell motility, tissue remodeling, metastasis, gene expression, cell survival, and proliferation.¹⁶ Paxillin undergoes tyrosine phosphorylation in response to various physiological stimuli and integrin-mediated cell adhesion events.⁴ Although a large number of stimuli induce tyrosine phosphorylation of

paxillin, only a few tyrosine kinases have been reported to phosphorylate paxillin, including the focal adhesion kinase (FAK), Src family kinases, the proto-oncogene c-Abl, Brk and Csk.^{4,16} Phosphorylation regulates adaptor molecule binding that ultimately coordinates multiple complex cell signaling pathways, including survival, proliferation, differentiation, migration, adhesion and invasion.^{4,16-18}

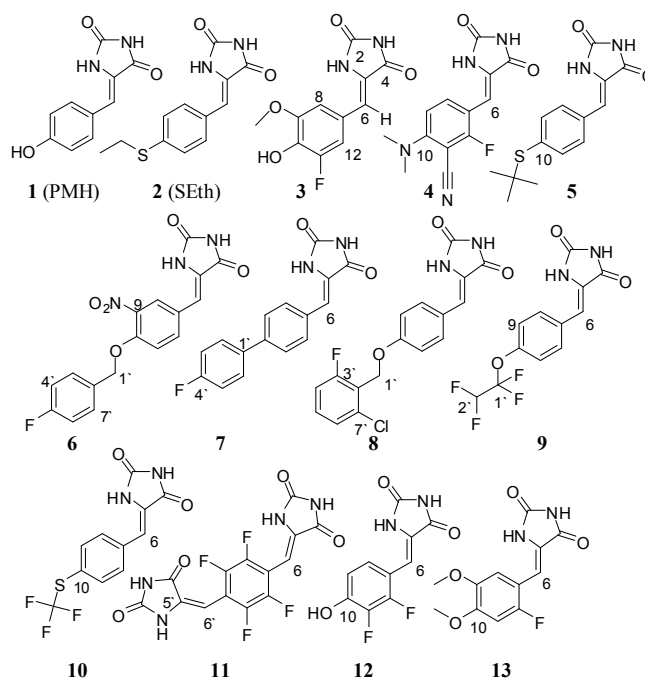
To improve cancer therapy, new potential therapeutic targets are required. The potential role of receptor and non-receptor tyrosine kinases, including c-Met, Brk and FAK, and their activation/overexpression in a variety of carcinomas, such as breast and prostate cancers, is of particular interest. Interfering with these kinases presents an attractive therapeutic strategy towards the management of those cancers.

Natural products have proven to be the most reliable source of new therapeutic entities.^{19,20} In the years 01/1981–12/2010, over 50% of the 1355 New Chemical Entities (NCEs) were natural products, natural product derivatives/analogs or synthetic compounds based on natural product pharmacophores making them the most consistently successful source of drug leads, both historically and currently.^{21,22} We previously reported the potent antiproliferative, antimigratory and anti-invasive properties of (Z)-5-(4-hydroxybenzylidene)-hydantoin (PMH, **1**, initially isolated from the marine sponge *Hemimycala arabica*) and a number of its semisynthetic and synthetic analogs against prostate cancer cells, PC-3 and PC-3M.²³⁻²⁶

The unique activities of PMHs were validated using several *in vitro* assays followed by *in vivo* testing in two mice models.²³⁻²⁶ The marine natural product **1** and its synthetic analog (Z)-5-(4-(ethylthio)benzylidene)-imidazolidine-2,4-dione (SEth, **2**) significantly increased transepithelial resistance (TER) of calcitonin (CT)-treated PC-3M cells, reversed CT action on TER, and abolished CT-induced increase in paracellular permeability of polarized PC-3M cell layers.^{23,24} Compounds **1** and **2** promoted tight junctions (TJs) formation and showed anti-invasive and antimigratory activities against metastatic prostate cancer cells in various *in vitro* assays. **1** and **2** showed prominent anti-metastatic activity in orthotopic xenograft of PC-3M cells in nude mice model, inhibiting tumor growth and formation of tumor micrometastases in distant organs.^{23,24} They also showed potent anti-metastatic activity in LPB-Tag transgenic mice model, reducing the growth of primary tumors and their metastasis in reproductive organs, decreasing morbidity and increasing mice survival average.²⁴ **1** and **2** reduced the total CD44 and CD44 v7-10 expression in PC-3M cells, which could partly justify their anti-metastatic activity.^{27,28} Activity levels (IC₅₀) of **1** and **2** were 139.2 and 51.4 μM, respectively. Subsequent optimizations afforded PMHs which inhibited the migration of PC-3 cells with IC₅₀ range of 4.2–21.8 μM.^{26,29} Multivariate analysis on PMHs was characterized by 14 physicochemical descriptors representing their lipophilicity, size, and electronic properties.²⁹ Inspection of variable importance projection (VIP) plot and descriptor's correlation coefficients revealed the importance of size and lipophilic parameters with the following order: MA (molecular area) < MV (molecular volume) < BC (bond count) < clog P. The MV, BC, and clog P were directly related to the activity, while MA was inversely related to the activity. The clog P and MV were the most influential descriptors.²⁹ CoMFA analysis of 35 synthetic PMHs revealed the following: 1. Areas of high steric bulk tolerance near the *p*-position of the benzylidene group in **2** were observed and therefore the activity can be significantly enhanced by bulky groups in this position. 2. Bulky groups are

sterically unfavorable near the *o*-positions and therefore it should not possess any bulky groups. 3. Electronegative (high electron density) groups, including alkyl substituted *O*, *N*, or *S* groups, near the *m*- and *p*-positions may show better activity. 4. Low electron density groups at the *o*-position can improve the activity.²⁹ A pharmacophore model for PMH's using DISTANCE Comparison technique (SYBYL's DISCOtech) was also reported.^{26,29} Pharmacophoric elements constructing this model included hydrogen-bond donor (HBD) atoms, hydrogen-bond acceptor (HBA) atoms, and hydrophobic centers. The final model with the highest score showed 3 HBA ligands, 2 HBD ligands, and 2 hydrophobic centers.^{26,29}

This study reports the synthesis of 11 new PMH analogs (**3-13**, Scheme 1) designed based on SAR features described above and their evaluation *in vitro* and *in vivo*. To expand the therapeutic scope of PMHs, the new compounds were additionally tested against the highly metastatic mammary MDA-MB-231 cancer cells. All compounds were tested in the MTT proliferation assay, wound-healing assay (WHA) and Cultrex® BME cell invasion assay. Western blot analysis for the most active **7** was conducted to evaluate possible molecular targets. A xenograft model was then selected using human breast cancer MDA-MB-231/GFP cells to assess the *in vivo* antitumor potential of **7**. To enhance its druglikeness and *in vivo* solubility, **7** was formulated using 5-hydroxypropyl-β-cyclodextrin (HPCD).



Scheme 1. Structures of the known and new PMHs **1-13**.

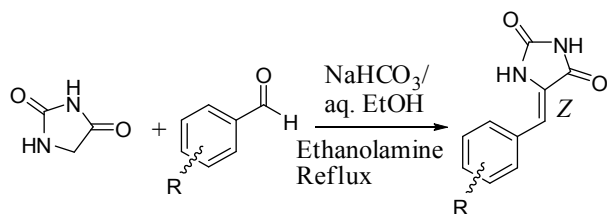
Results and discussion

1. Chemistry.

Using regioselective and cost-effective condensation reaction of hydantoin and substituted benzaldehydes,^{23,25,26} 11 new analogs of **1** were generated (**3-13**, Scheme 2). Generally, selected benzaldehydes had an electronegative group at the *para*-position possessing varying degree of bulkiness, with or without other substituents at the *ortho*- and/or *meta*-positions. A *para*-

positioned electronegative group was previously shown to be an essential mediator of the activity.^{23,26,29}

The HRESIMS data of **3** showed a molecular ion peak at m/z 251.0462 [M-H], suggesting the molecular formula $C_{11}H_9FN_2O_4$. ¹H and ¹³C NMR (Tables S1 and S4, Supplementary Information) indicated that **3** is (Z)-5-(9-methoxy-10-hydroxy-11-fluorobenzylidene)imidazolidine-2,4-dione. The olefinic proton singlet H-6 at δ_H 6.25 showed ³J-HMBC correlations with the amide carbonyl C-4 (δ_C 166.5) and the aromatic methine carbons C-8 and C-12 (δ_C 109.9 and 109.7, respectively), confirming the phenylmethylene hydantoin entity of **3**. Geometrical isomerism (*E/Z* isomers) would be possible around the exocyclic $\Delta^{5,6}$ system due to its restricted rotation. However, the used reaction condition regioselectively afforded the *Z*-geometry as confirmed by spectral data and previous literature.^{23,30,31} Generally, the use of *N*-unsubstituted hydantoins as a starting parent for the synthesis of PMHs usually afford their *Z*-isomer due to the greater steric repulsion in the *E*-analog.³⁰ Additionally, the chemical shift of the most diagnostic olefinic proton H-6 was downfield shifted in the ¹H NMR spectra (δ_H ~6.40 in most compounds), which further confirmed the *Z*-orientation of the $\Delta^{5,6}$ system. The expected chemical shift of H-6 in the *E*-PMHs would be more upfield shifted to ~6.20-6.30 ppm. The downfield shift of H-6 in the *Z*-PMHs is attributed to the anisotropic effect of the spatially near C-4 carbonyl group, which creates a deshielding cone.³¹ The ¹H and ¹³C NMR data of compounds **4-13** (Tables S1-S5, Supplementary Information) and their HRESIMS data were used to confirm their identity in a similar fashion.



Scheme 2. General synthetic scheme of phenylmethylene hydantoins.^{23,25,26,30}

2. Biological evaluation and structure-activity relationship (SAR)

2a. Cytotoxic activity against the non-tumorigenic MCF10A epithelial cell line. In order to determine the selective activity and cytotoxicity of the new compounds to malignant cells, MTT assay using the non-tumorigenic human breast cell line MCF10A was conducted. All compounds were nontoxic up to concentrations higher than their IC_{50} values in subsequent *in vitro* assays, suggesting their good selectivity towards the malignant cells (Figure 1, Table 1).

2b. Antiproliferative activity. In the proliferation assay, PMHs **6**, **7**, **10** and **11** showed the most promising activity in both prostate and breast cancer cell lines with IC_{50} values <10 μ M (Table 2). In MDA-MB-231 cells, **6** and **7** were the most active compounds, each with an IC_{50} value of 3.8 μ M. Both compounds possess either a *p*-fluoro substituted oxybenzyl ring (**6**) or a *p*-fluoro substituted phenyl (**7**) ring attached at the *para*-position of the benzylidene moiety. This additional ring may be involved in π - π stacking with the target receptor, thus anchoring the molecule in a pose that allows for better ligand-receptor interaction, hence better activity. The loss of *para*-fluoro substitution, compound **8**, caused a more drastic (almost five-fold) reduction in activity in

MDA-MB-231 cells than in PC-3 cells. On the other hand, bulkiness at the *para*-position, compounds **4**, **5** and **9**, had a more detrimental effect on the activity in PC-3 cells (Table 2). Compound **5** was active (IC_{50} 4.6 μ M) against the breast cancer MDA-MB-31 cells but only marginally active against PC-3 prostate cancer cells (IC_{50} 24.9 μ M). The known **2** proved to be more active (IC_{50} 8.8 μ M) against PC-3 cells than MDA-MB-231 cells (IC_{50} 18.8 μ M), whereas **1** was only marginally active (IC_{50} ~36.0 μ M) in both cell lines.

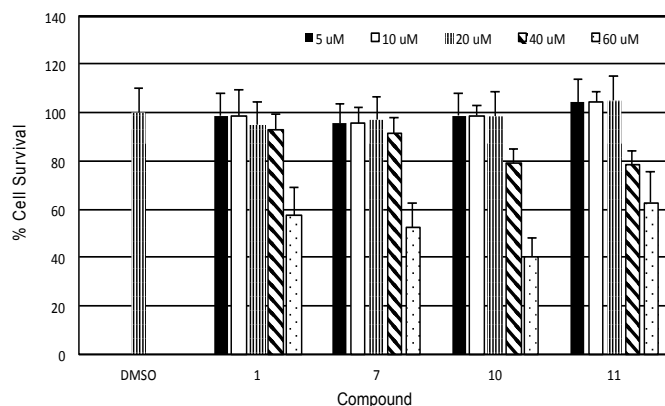


Figure 1. Selective cytotoxicity of the most active PMHs \pm SEM. PMHs **1**, **7**, **10**, and **11** showed no cytotoxicity to the non-tumorigenic human mammary epithelial cells MCF10A at concentrations up to 60 μ M. Error bars indicate the SEM for $n=3$ per compound.

Table 1. % Survival of normal mammary epithelial cells MCF10A treated with 40 μ M of each of PMHs **1-13**.

Compound	% Cell Survival (40 μ M)
1	92.9 \pm 6.5
2	88.6 \pm 8.2
3	90.5 \pm 5.3
4	87.6 \pm 8.9
5	92.0 \pm 7.1
6	89.3 \pm 9.2
7	91.5 \pm 6.4
8	78.4 \pm 3.7
9	92.1 \pm 11.1
10	79.3 \pm 5.6
11	78.6 \pm 5.4
12	86.1 \pm 7.9
13	85.0 \pm 6.4

2c. Antimigratory activity. In the wound-healing assay, compounds were more potent as PC-3 cell migration inhibitors, with most compounds showing IC_{50} values <15 μ M (Table 2). Compounds **7**, **10** and **11** showed the highest antimigratory activity with IC_{50} values of 1.3, 2.4, and 3.6 μ M, respectively (Table 2). The potency against MDA-MB-231 cells in the same assay was lower, based on their higher IC_{50} values (Table 2). Nevertheless, compound **7** was the most active with an IC_{50} of 15.9 μ M. This difference in potency can be attributed to various

reasons such as lower binding affinity to migration targets, binding to targets of lower importance to this particular cell line's migration or even different molecular targets dictating the migratory potential of these two cell lines.

Table 2. Antiproliferative and antimigratory activities of PMHs 1-13 against PC-3 and MDA-MB-231 cell lines.

Compound	Antiproliferative activity (IC ₅₀ , μM)		Antimigratory activity (IC ₅₀ , μM)	
	PC-3	MDA-MB-231	PC-3	MDA-MB-231
1	35.7	35.8	-	46.5
2	8.8	18.8	-	43.4
3	24.8	11.7	27.5	40.4
4	66.3	10.4	20.8	20.1
5	24.9	4.6	14.9	32.6
6	7.3	3.8	12.3	21.5
7	6.8	3.8	1.3	15.9
8	11.7	17.6	10.2	41.4
9	40.9	10.9	7.2	>50
10	6.5	9.6	2.4	>50
11	7.0	7.2	3.6	>50
12	17.2	18.4	19.4	16.1
13	38.0	13.4	5.3	>50

2d. Anti-invasive activity. The dose selected for testing in the Cultrex[®] BME cell invasion assay was based on the overall performance of compounds in the previous assays. 10 μM and 20 μM were selected as the optimal test doses for PC-3 and MDA-MB-231 cells, respectively. None of the compounds showed significant activity at the selected concentrations against PC-3 cells. Previous activity level of 1 and 2 in invasion assay models was >50 μM doses.^{23,24} In MDA-MB-231 cells, the most active compounds were 7 and 10 which allowed only 15.6 and 25.3% invasion, respectively.

2e. Western blot analysis. In Western blot analysis, compound 7 was evaluated against multiple targets following 72-hour treatment of MDA-MB-231 cells (Figure 2). Results showed that 7 caused a marked reduction of total c-Met and FAK protein expression and a subsequent reduction of their phosphorylated (active form) levels. The effect on total protein level may be related to the ability of the compound to either reduce the proteins expression (negatively) or enhance proteasomal degradation (positively). In addition, treatment with 7 showed a dose-response decrease in Brk, paxillin and Rac1 phosphorylation with no or little effect on their total levels. Inhibition of phosphorylation may be a consequence of upstream effects or direct interactions. These results are of significance since these proteins are strongly implicated in the pathophysiology of a variety of carcinomas, including breast and prostate cancers. Blocking one or more of these proteins is beneficial for the management of metastatic cancer forms.

2f. In vivo antitumor activity of 7. The new PMH analog 7 was considered the most promising hit and was further evaluated *in*

in vivo to assess its antitumor potential. An orthotopic nude mouse model was selected and the human breast cancer cell line MDA-MB-231/GFP was used. Because of solubility issues, 7 was formulated using hydroxypropyl β-cyclodextrin (HPCD).^{32,33} The formula (HPCD7) helped to improve 7's solubility based on the lack of precipitation in the animal peritoneum cavity upon intraperitoneal (i.p.) administration. Dosing (10 mg/Kg i.p., 3 times per week) started 5 days post-inoculation and continued for 4 weeks.

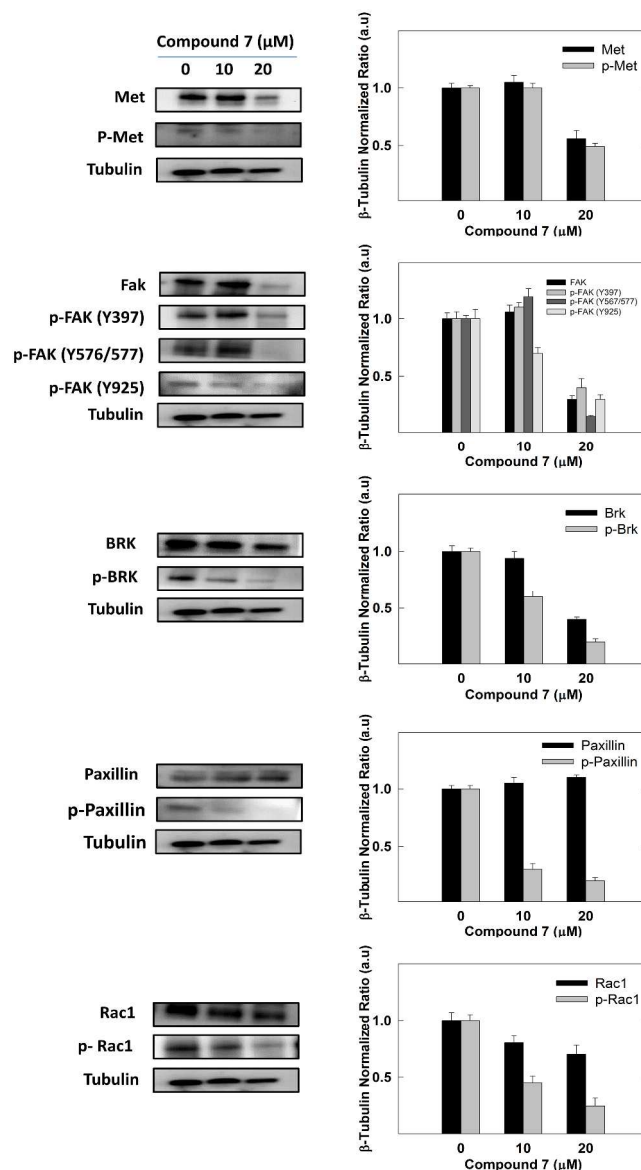


Figure 2. Western blot analysis of c-Met, phospho c-Met, FAK, phospho FAK, Brk, phospho Brk, paxillin, phospho paxillin, Rac1 and phospho Rac1 after exposure of MDA-MB-231 cells to 0, 10, and 20 μM treatments of 7 for 72 h. β-Tubulin was used as a loading control. Scanning densitometric analysis was performed on all blots done in triplicate and the integrated optical density of each band was normalized with corresponding β-tubulin, as shown in the bar graphs to the right of their respective Western blot images. Vertical bars in the graph indicate the normalized integrated optical density of bands visualized in each lane ± SEM

Growth of breast tumor was compared between non-treated animals (DMSO control group) and those receiving compound 7. Tumor progression was followed by direct measurement of tumor volume starting at day 14 post-inoculation. Figure 3a indicates that treatment with 7 slowed the progression of tumor and by the end of the 5-week study the average tumor volume in treatment group was about 50% of that in the DMSO control group. Moreover, treatment had no effect on mice weight or their gross phenotype, indicating that 7 did not exert toxic effects in treated mice (Figure 3b).

Immunohistochemical analysis showed that 7, when compared to the DMSO-control group, was capable of suppressing Ki-67 and CD-31 expression, indicating its ability to suppress both mitosis and new vessel formation, respectively (Figure 4, a and b). Ki-67 is a nuclear protein expressed only in proliferating cells, with peak concentrations in the G₂ and M phases of the cell cycle.^{34,35} CD-31 is a validated endothelial cell marker shown to be a sensitive and specific indicator of endothelial differentiation.^{33,35} In addition, 7 caused attenuation of p-Brk and p-FAK levels in tumor samples (Figure 4, c and d), further supporting the Western blot analyses results discussed earlier. These results strongly suggest the future potential of the PMH class, represented by 7, for use to control invasive breast cancer.

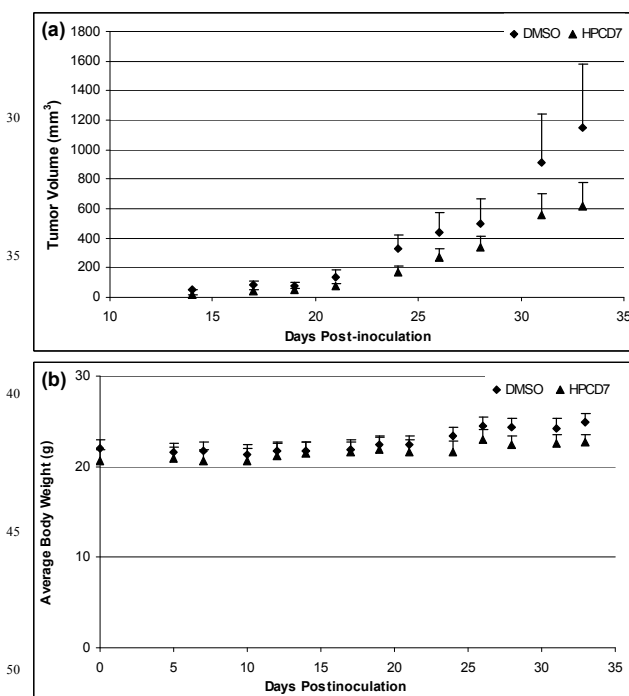


Figure 3. (a) *In vivo* activity of 7 formulated in HPCD. It slows the progression of tumor in an orthotopic nude mouse model as compared to the vehicle (DMSO) control. A paired-samples t-test was conducted to compare tumor volume in control group and HPCD7-treated group. A *p*-value of 0.0091 indicates a significant difference between the two groups. (b) No significant change in body weight was observed among treated animals, indicating the safety of the formulation. Error bars indicate standard error of the mean (SEM) for *n*=5.

Conclusions

Phenylmethylene hydantoin is an interesting prostate and breast cancer proliferation, migration and invasion inhibitory entity

inspired by marine natural products. The structural simplicity and synthetic feasibility of PMHs render them appropriate for future preclinical optimizations. This is the first report of activity of this class in breast cancer. The most active analog 7 showed promising *in vitro* and *in vivo* activities without notable toxicities. Its ability to interfere with multiple signaling pathways known to play a role in cancer metastasis qualifies it as interesting lead for future investigations.

Experimental

1. Chemicals, reagents, and antibodies

All materials were purchased from Sigma-Aldrich (St. Louis, MO), unless otherwise stated. All antibodies were purchased from Cell Signaling Technology (Beverly, MA), unless otherwise stated. Antibody for Brk was obtained from Abnova (Walnut, CA). Antibody for p-Brk was purchased from Santa Cruz Biotechnology (Santa Cruz, CA). Goat anti-rabbit and goat anti-mouse secondary antibodies were purchased from PerkinElmer Biosciences (Boston, MA). Hepatocyte growth factor (HGF) was purchased from PeproTech Inc., (Rocky Hill, NJ).

2. General experimental procedures

TLC analysis was carried on precoated Si gel 60 F₂₅₄ 500 μm TLC plates (EMD Chemicals), and CHCl₃/MeOH (9:1) was used as the developing system. ¹H and ¹³C NMR spectra were recorded in DMSO-*d*₆ on a JEOL Eclipse-ECS NMR spectrometer operating at 400 MHz for ¹H NMR and 100 MHz for ¹³C NMR. High-resolution ESIMS experiments were conducted using a JEOL JMS-T100 LP AccuTOF LC-Plus, equipped with an ESI source (JEOL Co. Ltd., Tokyo, Japan). ESI-MS detection was set using negative ion mode; needle voltage set at -2,000 V; and the ring lens and orifice 1 and 2 voltages set at -10, -35, and -7 V, respectively. Nitrogen was used as the nebulizing and desolvation gas, and pressure was maintained constant at 0.608 MPa. Desolvation chamber and orifice 1 temperatures were set to 250 °C and 120 °C, respectively. Results were obtained using Mass Center software, MS-56010MP (JEOL).

3. Chemical synthesis

3.1. Preparation of synthetic PMHs^{23,25,31}

A two-neck round bottom flask was used to dissolve hydantoin (1.0 g) in 10 mL H₂O by heating at 70 °C in an oil bath with continuous stirring. A saturated solution of NaHCO₃ was used to maintain the pH at 7.0. Ethanolamine (0.9 mL) was then added and the temperature raised to 90 °C. An equimolar quantity of substituted benzaldehyde dissolved in 10 mL EtOH was then added dropwise. The mixture was kept under reflux for 10 h. The reaction was monitored by TLC every hour and the endpoint of the reaction was visualized by the formation of a precipitate. The mixture was then cooled to 4 °C, and the precipitate was filtered, washed with EtOH/H₂O (1:5), and then recrystallized from EtOH. Yields of the product ranged from 60–90%, based on the nature of the individual benzaldehyde used.

3.2. (Z)-5-(9-methoxy-10-hydroxy-11-fluorobenzylidene)-imidazolidine-2,4-dione (3)

Yellow amorphous solid, ¹H and ¹³C NMR see Tables S1 and S4 in Supplementary Information; HRESIMS *m/z* 251.0462 [M-H]⁻ (calcd for C₁₁H₈FN₂O₄, 251.0468).

3.3. (Z)-5-(10-(dimethylamino)-11-cyano-12-fluorobenzylidene)imidazolidine-2,4-dione (4)

White amorphous solid, ¹H and ¹³C NMR see Tables S1 and S4

in Supplementary Information; HRESIMS m/z 273.0783 $[M-H]^-$ (calcd for $C_{13}H_{10}FN_4O_2$ 273.0788).

3.4. (Z)-5-(10-(tert-butylthio)benzylidene)imidazolidine-2,4-dione (5)

Yellow amorphous solid, 1H and ^{13}C NMR see Tables S1 and S4 in Supplementary Information; HRESIMS m/z 275.0850 $[M-H]^-$ (calcd for $C_{14}H_{15}N_2O_2S$ 275.0854).

3.5. (Z)-5-(9-nitro-10-(5'-fluorobenzyloxy)benzylidene)imidazolidine-2,4-dione (6)

Yellow amorphous solid, 1H and ^{13}C NMR see Tables S1 and S4 in Supplementary Information; HRESIMS m/z 356.0689 $[M-H]^-$ (calcd for $C_{17}H_{11}FN_3O_5$ 356.0683).

15

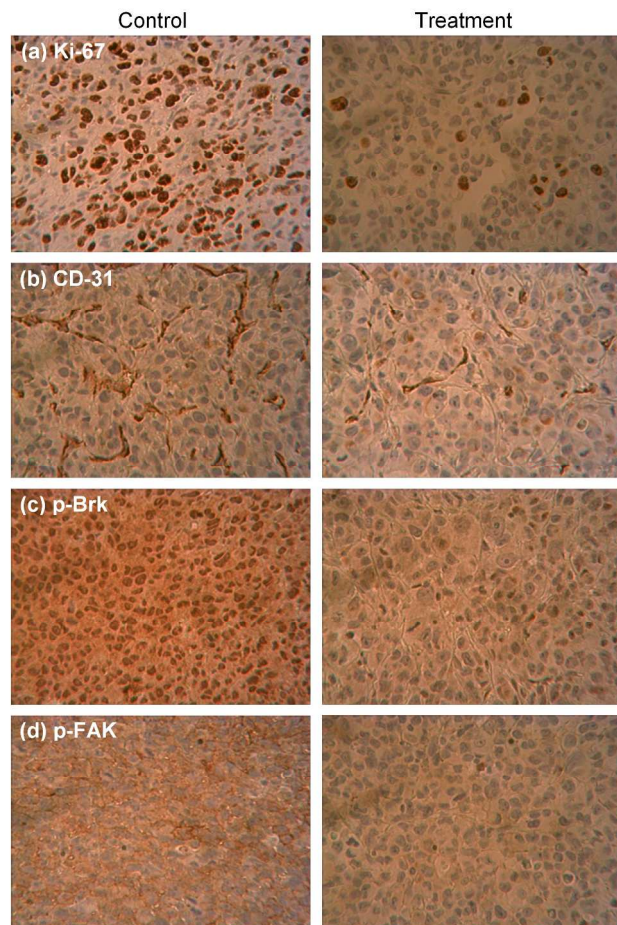


Figure 4. Immunostaining of sections obtained from vehicle-treated (control) and 7-treated (10 mg/kg/day, 3 X/week) mice against Ki-67 (mitosis marker), CD31 (endothelial marker), p-Brk and p-FAK antibodies.

3.6. (Z)-5-((4'-fluorobiphenyl-10-yl)methylene)imidazolidine-2,4-dione (7)

Yellow amorphous solid, 1H and ^{13}C NMR see Tables S1 and S4 in Supplementary Information; HRESIMS m/z 281.0724 $[M-H]^-$ (calcd for $C_{16}H_{10}FN_2O_2$ 281.0726).

3.7. (Z)-5-(10-(3'-fluoro-7'-chlorobenzyloxy)benzylidene)imidazolidine-2,4-dione (8)

White amorphous solid, 1H and ^{13}C NMR see Tables S2 and S4 in Supplementary Information; HRESIMS m/z 345.0448 $[M-H]^-$ (calcd for $C_{17}H_{11}ClFN_2O_3$ 345.0442).

3.8. (Z)-5-(10-(1',1',2',2'-tetrafluoroethoxy)benzylidene)imidazolidine-2,4-dione (9)

White amorphous solid, 1H and ^{13}C NMR see Tables S2 and S5 in Supplementary Information; HRESIMS m/z 303.0397 $[M-H]^-$ (calcd for $C_{12}H_9F_4N_2O_3$ 303.0393).

3.9. (Z)-5-(10-(trifluoromethylthio)benzylidene)imidazolidine-2,4-dione (10)

Yellow amorphous solid, 1H and ^{13}C NMR see Tables S2 and S5 in Supplementary Information; HRESIMS m/z 287.0107 $[M-H]^-$ (calcd for $C_{11}H_6F_3N_2O_2S$ 287.0102).

3.10. (5Z,5'E)-5,5'-(perfluoro-7,10-phenylene)bis(methan-1-yl-1-ylidene)diimidazolidin e-2,4-dione (11)

Yellow amorphous solid, 1H and ^{13}C NMR see Tables S2 and S5 in Supplementary Information; HRESIMS m/z 369.0249 $[M-H]^-$ (calcd for $C_{14}H_5F_4N_4O_4$ 369.0247).

3.11. (Z)-5-(10-hydroxy-11,12-difluorobenzylidene)imidazolidine-2,4-dione (12)

Yellow amorphous solid, 1H and ^{13}C NMR see Tables S3 and S5 in Supplementary Information; HRESIMS m/z 239.0263 $[M-H]^-$ (calcd for $C_{10}H_5F_2N_2O_3$ 239.0268).

3.12. (Z)-5-(9,10-dimethoxy-12-fluorobenzylidene)imidazolidine-2,4-dione (13)

Yellow amorphous solid, 1H and ^{13}C NMR see Tables S3 and S5 in Supplementary Information; HRESIMS m/z 265.0621 $[M-H]^-$ (calcd for $C_{12}H_{10}FN_2O_4$ 265.0625).

4. In vitro activities

All cell lines, prostate cancer PC-3, breast cancer MDA-MB-231 and normal breast MCF10A, were purchased from ATCC (Manassas, VA). PC-3 and MDA-MB-231 cells were maintained in RPMI 1640 medium (GIBCO-Invitrogen, NY) supplemented with 10% fetal bovine serum (FBS) and glutamine (2 mmol/L), and containing penicillin G (100 U/mL), and streptomycin (100 μ g/mL). MCF10A cells were maintained in Dulbecco's modified Eagle's medium (DMEM)/F12 containing 5% horse serum, 1% penicillin/streptomycin, 0.5 μ g/mL hydrocortisone, 100 ng/mL cholera toxin, 10 μ g/mL insulin, and 20 ng/mL epidermal growth factor (rhEGF). Cells were incubated at 37°C in a humidified incubator under 5% CO_2 .

A stock solution of each compound was prepared in DMSO at a concentration of 25 mM for all assays. Appropriate media (serum-free, 0.5% FBS or 5% FBS) were used to prepare compounds at their final concentrations for each assay. The vehicle (DMSO) control was prepared by adding the maximum volume of DMSO used in preparing test compounds to the appropriate media type such that the final DMSO concentration never exceeded 0.2%.

4.1. MTT (proliferation assay)

The antiproliferative activity of test compounds was evaluated on the human prostate cancer cell line PC-3 and the breast cancer cell line MDA-MB-231 using the procedure described previously.^{36,37} Briefly, cells in exponential growth were plated in a 96-well plate at a density of 1×10^4 cells per well (6 wells/group), and allowed to attach overnight at 37°C under 5% CO_2 in a humidified incubator. Complete growth medium was then replaced with 100 μ L of RPMI media (GIBCO-Invitrogen, NY) supplemented with 5% FBS, containing various doses of the specific test compound and incubation resumed at 37°C under 5% CO_2 for 72 h. Cells in all groups were fed fresh treatment media every other day. Viable cell count was determined using the 3-

(4,5-dimethylthiazol-2-yl)-2,5-diphenyl tetrazolium bromide (MTT) colorimetric assay.³⁸ The absorbance of each sample was measured at λ 570 nm on a microplate reader (BioTek, VT, USA). The number of cells per well was calculated against a standard curve prepared at the start of each experiment by plating various numbers of cells (in the range 1,000-60,000 cells per well), as counted by a hemocytometer. The IC₅₀ value for each compound was calculated by nonlinear regression (curve fit) of log (concentration) versus the % survival, implemented in GraphPad Prism version 5.0 (GraphPad Software, La Jolla, CA, USA). The % cell survival was calculated as follows: % cell survival = (Cell No._{treatment}/Cell No._{DMSO}) x 100%.

4.2. Wound-healing assay (WHA)

The WHA is a simple method for evaluating directional cell migration *in vitro*.³⁹ The assay was conducted as described previously.³⁸ Briefly, cells were plated in sterile 24-well plates and allowed to form a confluent monolayer per well (>90% confluence) overnight. Wounds were then inflicted in each cell monolayer using a sterile 200 μ L pipette tip. Media was removed and cells were washed twice with PBS and once with fresh RPMI media. Test compounds at the desired concentrations were prepared in fresh media (0.0% or 0.5% FBS) and were added to wells in triplicate. The incubation was carried out for 24 h, after which media was removed and cells were washed, fixed and stained using Diff-Quick™ staining (Dade Behring Diagnostics, Aguada, Puerto Rico). Cells which migrated across the inflicted wound were counted under the microscope in at least five randomly selected fields (magnification: 400X).

4.3. Cultrex® BME cell invasion assay

This assay was conducted according to the protocol provided with the kit.⁴⁰ Briefly, about 50 μ L of basement membrane extract (BME) coat (1X for MDA-MB-231 and 0.5X for PC-3 cells) was added per well. After overnight incubation at 37°C in a 5% CO₂, 50,000/50 μ L of cells in fresh RPMI medium was added per well to the top chamber. Test compounds were prepared at 6X the desired concentrations (60 and 120 μ M) and 10 μ L of each compound was added in triplicate to achieve the final test concentrations (10 and 20 μ M). 150 μ L of RPMI medium, containing 10% FBS and penicillin/streptomycin as well as fibronectin (1 μ L/mL) and *N*-formyl-met-leu-phe (10 nM) as chemoattractants, was then added to the lower chamber. Plates were re-incubated at 37°C in 5% CO₂ for 24 h after which the top and bottom chambers were aspirated and washed with wash buffer supplemented with the kit. 100 μ L of cell dissociation/calcein-AM solution was added to the bottom chamber and incubated at 37°C in 5% CO₂ for 1 h. The cells internalize calcein-AM, and the intracellular esterases cleave the acetomethylester (AM) moiety to generate free calcein. Fluorescence of the samples was determined at $\lambda_{excitation}$ 485 nm and $\lambda_{emission}$ 528 nm using an ELISA plate reader (BioTek, VT, USA). The numbers of cells that invaded through the BME coat were calculated using a standard curve and % invasion of different treatments was compared relative to the DMSO control.

4.4. Western blot analysis

Western blot analysis was performed according to the method previously described.⁴¹ Briefly, MDA-MD-231 cells were initially plated at a density of 1x10⁶ cells/100mm culture plate, allowed to attach overnight in RPMI-1640 media containing 10% FBS. Cells were then washed with PBS and incubated with vehicle control or treatment in serum-free media for 3 days in culture. At the end of treatment period, cells were lysed in RIPA buffer (Qiagen Sciences Inc., Valencia, CA). Protein

concentration was determined by the BCA assay (Bio-Rad Laboratories, Hercules, CA). Equivalent amounts of protein were electrophoresed on SDS-polyacrylamide gels. The gels were then electroblotted onto PVDF membranes. These PVDF membranes were then blocked with 2% BSA in 10 mM Tris-HCl containing 50 mM NaCl and 0.1% Tween 20, pH 7.4 (TBST) and then, incubated with specific primary antibodies against Brk (Abnova, CA) and p-Brk (Santa Cruz, CA) and incubated overnight at 4°C. At the end of incubation period, membranes were washed 5 times with TBST and then incubated with respective horseradish peroxidase-conjugated anti-rabbit or anti-mouse secondary antibodies (PerkinElmer Biosciences, MA) in 2% BSA in TBST for 1-h at room temperature followed by rinsing with TBST 5 times. Blots were then visualized by chemiluminescence according to the manufacturer's instructions (Pierce, Rockford, IL, USA). Images of protein bands from all treatment groups within a given experiment were acquired using Kodak Gel Logic 1500 Imaging System (Carestream Health Inc, New Haven, CT, USA). The visualization of β -tubulin (Cell Signaling Technology, MA) was used to ensure equal sample loading in each lane. All experiments were repeated at least three times and a representative Western blot image from each experiment is shown in Figure 2.

4.5. Xenograft studies⁴²

All animal experiments were approved by the Institutional Animal Care and Use Committee, University of Louisiana at Monroe, and were handled in strict accordance with good animal practice as defined by the NIH guidelines. Athymic nude mice (Foxn1nu/Foxn1+, 4-5 weeks, female) were purchased from Harlan (Indianapolis, IN). Mice had free access to drinking water and pelleted rodent chow (no.7012, Harlan/Teklad, Madison, WI) and were acclimated to animal house facility conditions at a temperature of 18–25°C, with a relative humidity of 55 to 65% and a 12 h light/dark cycle, for at least one week prior to the experiments. MDA-MB-231/GFP human breast cancer cells were cultured and resuspended in serum-free DMEM medium. After anesthesia, cell suspensions (1x10⁶ cells/20 μ L) were inoculated into the second mammary gland fat pad just beneath the nipple of each animal to generate orthotopic breast tumors. At 48 h post-inoculation, the mice were randomly divided into two groups: i) the vehicle-treated control group (n=5), and ii) the HPCD7-treated group (n=5). Treatment (3X/ week) started 5 days postinoculation with intraperitoneal (i.p.) administered vehicle control (DMSO / saline) or 10 mg/kg HPCD7. HPCD7 formula was prepared as follows: 4 g of hydroxypropyl β -cyclodextrin was dissolved in 20 mL distilled water (1:5 ratio). Compound 7 was then added to this solution, the vial sealed and autoclaved for 15-30 minutes to achieve a final concentration of 0.5 mg/mL. Mice were monitored daily for general wellbeing, and tumor volume and body weight were measured prior to each dose (3X/week). Tumor volume (V) was calculated using the formula $V = (L \times W^2)/2$, where L is the length in mm and W is the width in mm of tumors as measured using a caliper. All mice were sacrificed on day 33 postinoculation, and the tumors were excised and weighed. Some tumor tissues were stored at -80°C until total protein extraction for Western blot analysis and others stored in 70% ethanol at RT for immunohistochemistry studies.

4.6. Immunohistochemistry

The tumor specimens were processed with the use of alcohols and xylene and then infiltrated in paraffin wax using the Excelsior™ ES Tissue Processor. Paraffin sections were dewaxed in xylene, rinsed in grade alcohol, and rehydrated in water and then were placed in citric buffer (PH 6.0) and treated in a microwave oven

with high power for 3 min and 10% goat serum for 30 min. Subsequently, antibodies with proper dilution were applied on the sections as follows: CD31 (Pierce Product #PA5-32321; 1:50 dilution, 1h at RT), Ki-67 (Cell Signalling Product #9027; 1:150 dilution, 1h at rt), p-Brk (Bioss Product # bs-12890R; 1:100, 1h at rt), and p-FAK (Cell Signalling Product #8556; 1:100, 1h at rt). Following that, secondary antibodies (Ventana Multimer Anti Rb-HRP Product #760-4311 24 min at rt) were applied. Signals were developed with Vector ImmPACT DAB Product #SK-4105 for 8 min at rt. The sections were finally counter stained by hematoxylin solution for 1 min at rt.

Acknowledgments

The Louisiana Campuses Research Initiative (LaCRI) is acknowledged for the financial support (ELD041). The Louisiana Board of Regents is also acknowledged for the support of the new HRMS facility (LEQSF(2013-14)-ENH-TR-26).

Notes and references

*To whom correspondence should be addressed. Tel: 318-342-1725. Fax: 318-342-1737. E-mail: elsayed@ulm.edu

^aDepartment of Basic Pharmaceutical Sciences, School of Pharmacy, University of Louisiana at Monroe, Monroe, Louisiana 71201 USA.

^bDepartment of Toxicology, School of Pharmacy, University of Louisiana at Monroe, Monroe, Louisiana 71201 USA.

- (a) American Cancer Society. www.cancer.org (Accessed January, 30th 2014). (b) R. Siegel, J. Ma, J. Zou and A. Jemal. *CA: Cancer J. Clin.*, 2014, **64**, 9-29.
- H. Yu, X. Li, S. Sun, X. Gao and D. Zhou, *Biochem. Biophys. Res. Commun.*, 2012, **427**, 659.
- J. R. Sierra and M. S. Tsao, *Ther. Adv. Med. Oncol.*, 2011, **3**, S21.
- H. Y. Chen, C. H. Shen, Y. T. Tsai, F. C. Lin, Y. P. Huang and R. H. Chen, *Mol. Cell. Biol.*, 2004, **24**, 10558.
- K. P. Raghav, W. Wang, S. Liu, M. C. Chavez-MacGregor, X. Meng, G. N. Hortobagyi, G. B. Mills, F. Meric-Bernstam, G. R. Blumenschein and A. M. Gonzalez-Angulo, *Clin. Cancer Res.*, 2012, **18**, 2269.
- W. H. Tu, C. Zhu, C. Clark, J. G. Christensen and Z. Sun, *BMC Cancer*, 2010, **10**, 556.
- J. D. Holland, B. Györfy, R. Vogel, K. Eckert, G. Valenti, L. Fang, P. Lohneis, S. Elezkurtaj, U. Ziebold and W. Birchmeier, *Cell Reports*, 2013, **5**, 1214.
- P. J. Mitchell, K. T. Barker, J. Shipley and M. R. Crompton, *Oncogene*, 1997, **15**, 1497.
- M. Aubele, G. Auer, A. K. Walch, A. Munro, M. J. Atkinson, H. Braselmann, T. Fornander and J. M. S. Bartlett, *Br. J. Cancer*, 2007, **96**, 801.
- T. M. Regan Anderson, D. L. Peacock, A. R. Daniel, G. K. Hubbard, K. A. Lofgren, B. J. Girard, A. Schörg, D. Hoogewijs, R. H. Wenger, T. N. Seagroves and C. A. Lange, *Cancer Res.*, 2013, **73**, 5810.
- Y. Zheng, Z. Wang, W. Bie, P. M. Brauer, B. E. Perez White, J. Li, V. Nogueira, P. Raychaudhuri, N. Hay, D. A. Tonetti, V. Macias, A. Kajdacsy-Balla and A. L. Tyner, *Cancer Res.*, 2013, **73**, 5426.
- T. R. Johnson, L. Khandrika, B. Kumar, S. Venezia, S. Koul, R. Chandhoke, P. Maroni, R. Donohue, R. B. Meacham and H. K. Koul, *Mol. Cancer Res.*, 2008, **6**, 1639.
- T. Heinrich, J. Seenisamy, L. Emmanuvel, S. S. Kulkarni, J. Bomke, F. Rohdich, H. Greiner, C. Eudar, M. Krier, U. Grädler and D. Musil, *J. Med. Chem.*, 2013, **56**, 1160.
- Y. C. Chang, P. N. Chen, S. C. Chu, C. Y. Lin, W. H. Kuo and Y. S. Hsieh, *J. Agric. Food Chem.*, 2012, **60**, 8395.
- J. K. Slack, R. B. Adams, J. D. Rovin, E. A. Bissonette, C. E. Stoker and J. T. Parsons, *Oncogene*, 2001, **20**, 1152.
- A. Sen, K. O'Malley, Z. Wang, G. V. Raj, D. B. DeFranco and S. R. Hammes, *J. Biol. Chem.*, 2010, **285**, 28787.
- M. D. Schaller, *Oncogene*, 2001, **20**, 6459.
- K. R. Legate, S. A. Wickström and R. Fässler, *Genes Dev.*, 2009, **23**, 397.
- K. H. Lee, *J. Nat. Prod.*, 2010, **73**, 500.
- K. V. Sashidhara, K. N. White and P. Crews, *J. Nat. Prod.*, 2009, **72**, 588.
- A. L. Harvey, *Revista de Salud. Animal*, 2009, **31**, 8.
- D. J. Newman and G. M. Cragg, *J. Nat. Prod.*, 2012, **75**, 311.
- M. Mudit, M. Khanfar, A. Muralidharan, S. Thomas, G. V. Shah and K. A. El Sayed, *Bioorg. Med. Chem.*, 2009, **17**, 1531.
- G. V. Shah, A. Muralidharan, S. Thomas, M. Gokulgandhi, M. Mudit, M. Khanfar and K. A. El Sayed, *Mol. Cancer Ther.*, 2009, **8**, 509.
- M. Khanfar, B. Abu Asal, M. Mudit, A. K. Kaddoumi and K. A. El Sayed, *Bioorg. Med. Chem.*, 2009, **17**, 6032.
- M. Mudit and K. A. El Sayed, *Chem. Biod.*, 2011, **8**, 1470-1485.
- K. Yang, Y. Tang and K. A. Iczkowski, *Am. J. Tran. Res.*, 2010, **2**, 88-94.
- K. A. Iczkowski, *Am. J. Tran. Res.*, 2011, **3**, 1-7.
- M. K. Khanfar and K. A. El Sayed, *Eur. J. Med. Chem.*, 2010, **45**, 5397-5405.
- E. Kleinpeter, *Struct. Chem.*, 1997, **8**, 161-173.
- J. C. Thenmozhiyal, P. T. Wong and W.K. Chui, *J. Med. Chem.*, 2004, **47**, 1527-1535
- K. H. Frömring and J. Szejtli. Pharmacokinetics and Toxicology of Cyclodextrins. In: Cyclodextrins in Pharmacy, Springer Netherlands: 1994, Chapter 3, pp. 33-44.
- N. Özdemir and J. Erkin, *Drug Dev. Ind. Pharm.*, 2012, **38**, 331.
- J. S. Hardwick, Y. Yang, C. Zhang, B. Shi, R. McFall, E. J. Koury, S. L. Hill, H. Dai, R. Wasserman, R. L. Phillips, E. J. Weinstein, N. E. Kohl, M. E. Severino, J. R. Lamb and L. Sepp-Lorenzino, *Mol. Cancer Ther.*, 2005, **4**, 413.
- Ö. Yerebakan, M. A. Çifticioğlu, B. K. Akkaya and E. Yilmaz, *J. Dermatol.*, 2003, **30**, 33.
- A. A. Sallam, S. Ramasahayam, S. A. Meyer and K. A. El Sayed, *Bioorg. Med. Chem.*, 2010, **18**, 7446.
- A. A. Sallam, N. M. Ayoub, A. I. Foudah, C. R. Gissendanner, S. A. Meyer and K. A. El Sayed, *Eur. J. Med. Chem.*, 2013, **70**, 594.
- Trevigen, Inc., TACS MTT Assays: Cell Proliferation and Viability Assays, 2003, pp. 2-7.
- L. G. Rodriguez, X. Wu and J. L. Guan, *Methods Mol. Biol.*, 2005, **294**, 23.
- Cultrex[®] BME cell invasion assay protocol. www.trevigen.com (accessed 12.01.13).
- M. R. Akl, N. M. Ayoub, B. S. Abuasal, A. Kaddoumi and P. W. Sylvester, *Fitoterapia*, 2013, **84**, 347.
- K. Bhingre, V. Gupta, S. Hosain, S. D. Satyanarayanajois, S. A. Meyer, B. Blaylock, Q. J. Zhang and Y. Y. Liu, *Int J Biochem Cell Biol.*, 2012, **44**, 1770.